Cross-shaped markers for the preparation of site-specific transmission electron microscopy lamellae using focused ion beam techniques

T. J. O'Hanlon, A. Bao, F. C.-P. Massabuau, M. J. Kappers and R. A. Oliver

Abstract

We describe the use of a cross-shaped platinum marker deposited using electron-beam-induced deposition (EBID) in a focused ion beam – scanning electron microscope (FIB-SEM) system to facilitate site-specific preparation of a TEM foil containing a trench defect in an InGaN/GaN multiple quantum well structure. The defect feature is less than 100 nm wide at the surface. The marker is deposited prior to the deposition of a protective platinum strap (also by EBID) with the centre of the cross indicating the location of the feature of interest, while the arms of the square cross make an acute angle of 45° with the strap's long axis. During the ion-beam thinning process, the marker may be viewed in cross-section from both sides of the sample alternately, and the coming together of the features relating to the arms of the cross indicates increasing proximity to the feature of interest. Although this approach does allow increased precision in locating the region of interest during thinning, it also increases the time required to complete the sample preparation. Hence, this method is particularly well suited to directly correlated multi-microscopy investigations in previously characterised material where high yield and the precise location are more important than preparation time. In addition to TEM lamella preparation, this method could equally be useful for preparing site-specific atom probe tomography (APT) samples.

Introduction

Focused ion beam microscopes are well-established, powerful tools for microscale and nanoscale sample manipulation. Their efficacy in the preparation of high quality, thin lamellae for transmission electron microscopy (TEM) investigations is well known, with the site-specificity they offer being one of their principal advantages in this context. Dual scanning electron- and ion-beam instruments

(known as FIB-SEMs) combined the ion-beam's milling capabilities with the sharper, less destructive imaging of the electron-beam, extending their capability. Furthermore, the inclusion of an in-situ gas injection system (GIS) allowed precise electron- or ion-beam-induced deposition (EBID and IBID) and micromanipulator systems facilitated in-situ sample transfer. Combined, these yielded a powerful and flexible route for high quality TEM sample preparation from specific areas. With these tools, site-specific samples may be produced with an accuracy of ≈ 20 nm for gallium FIB-SEMs[1] and milling accuracies for structures produced in helium ion systems are below[2] 5 nm. However, for nanoscale features without clear contrast to their cross section, or with densely packed features easily mistaken for one another, achieving site specificity during the thinning stages of preparation becomes more challenging. Sample charging, beam drift and the need for thin final TEM samples compound the issue: markers are needed to ensure the coincidence of the region of interest (ROI) and the final prepared lamella.

Site-specific preparation of sub-100 nm regions in the FIB/SEM is also important for atom probe tomography (APT) samples. APT specimens are prepared as long needles with a final radius of curvature of 25 - 100 nm, which are thinned down in the FIB/SEM with a series of concentric annular milling patterns[3] at progressively lower ion beam currents and/or voltages before finally removing most of the platinum layer with a low voltage FIB clean-up step[4]. Site-specific features such as grain boundaries, surface cracks, and nanoscale extended defects are frequent candidates for study by APT[5–7]: marker strategies could greatly assist in ensuring features which are difficult to locate during the thinning process are contained within the final needle specimens.

Another driving force for improving the control of site specificity is in the directly correlated imaging between different kinds of microscopes, often termed multi-microscopy[7,8]. A TEM specimen may need to be prepared from an area with interesting electrical or optical properties but without clear contrast in the FIB-SEM, particularly during cross-sectional thinning, with the ROI located in plan-view relative to nearby surface features or debris. In this case too, a method of marking the ROI location during the preparation and thinning of TEM samples is required.

Fiducial markers are commonly used either side of the selected region during the automated preparation of TEM lamellae, allowing the software to locate the ROI and compensate for drift effects[9–11]. However, as these markers are outside the prepared lamella, they cannot guide the final thinning stages in the in-situ lift-out process. Small, low contrast features may be lost during the final thinning stages, or the wrong feature may be chosen from a dense population of similar features

(important for directly correlated microscopy). Where the lamellae are thinned as much as possible prior to lift-out (as in a typical ex-situ lift-out process) the risk of damaging or losing the sample is increased and the lamella cannot be returned to the instrument for further thinning[12]. The resulting reduced yield becomes more serious for multi-microscopy experiments, where significant time may have already been invested in investigating a specific nanoscale feature. Similarly, if a rare or unusual feature is under investigation, losing or damaging the sample may be particularly problematic. Markers which were present *inside* the lamellae throughout the whole thinning process, conversely, would ensure the final film contains or bisects the desired features, by allowing the ROI position to be tracked throughout the entire preparation process.

Markers contained in a lamella after lift-out have previously been demonstrated by Pettersson et al. using trenches milled perpendicularly to the lamellar long axis either side of protective platinum strap[13]. However, a number of aspects of this method may reduce its efficacy for certain samples. Firstly, a protective cap is needed to protect the sample during marker milling. This could obscure small features, making the correct positioning of markers more difficult, especially if the sample has drifted during deposition. Secondly, it is hard to gauge the depth into the lamella of the ROI from the sidewalls during the final thinning, which may make it more difficult to ensure small volumes are contained in the finished TEM film. In addition, the trenches cannot be milled very close to the desired region, or the material would be damaged. Finally, as material either side of the ROI is necessarily lost or damaged where the trenches are milled, comparisons with the surrounding material would be impeded. For APT preparation, markers based on trenches milled around the ROI after the deposition of protective platinum layer have also been demonstrated[14], but the potential drawbacks of using milled markers detailed above would similarly apply to their use in the preparation of APT samples.

Recent advances in automated TEM preparation routines have started to address this problem. For example, the AutoTEM 4 software[15] from Thermo-Fisher includes an automated TEM sample preparation routine in which a fiducial marker is milled through the protective cap at one end of the lamella to allow automation of the final thinning stages. However, such automated routines are not available across all instruments and may lack the flexibility to be extended into sample preparation for other microscopy techniques such as APT. Automated routines are in general also less adaptable to the user's needs and may fail in circumstances where a user operating a more manual technique could take appropriate corrective action, such as when a lamella bends or otherwise distorts upon thinning.

An alternative marker strategy is presented here, with cross-shaped markers produced solely by deposition. These markers were placed directly over the ROI without damage to this or the surrounding region and were present throughout the entire thinning process. Crucially, the half-spacing of the marker contrast – visible on the thinning sidewalls – gave the distance of the ROI from the exposed milled surface on either side. These markers allowed previously characterised nanoscale features to be located and centred in thin FIB-prepared lamellae, bisecting a region only 60 nm wide (at its narrowest point). Directly correlated TEM measurements could subsequently be carried out on the exact same feature, facilitating the multi-microscopy process.

Materials and methods

Extended defects are particularly prevalent in heteroepitaxially-grown III-N semiconductors, and the ability to isolate particular defects for further investigation by TEM or atom probe tomography, using a multi-microscopy approach, has been shown to provide useful insights otherwise difficult to obtain[7,16–19]. Hence, we use here a sample of multiple quantum wells (QWs) grown on a GaN-on-sapphire template to demonstrate this marker method. The sample exhibited trench defects at the surface. These 3D features in InGaN/GaN QW structures comprise an open trench partially or fully enclosing material with differing emission properties from the surrounding material. They are initiated by a sub-surface basal-plane stacking fault (BSF) which is connected to the open trench at the surface by a stacking mismatch boundary (SMB)[20]. The link between the morphology, structure and emissive properties of these nanoscale features is not straightforward, making them an ideal candidate for directly correlated analysis by multiple microscopy techniques.

The sample was grown by metal-organic vapour phase epitaxy in a Thomas Swan 6 × 2 inch close-coupled showerhead reactor. A c-plane sapphire substrate was used with a miscut of (0.25±0.10)° towards (11-20). Firstly, a GaN pseudo-substrate was grown, with approx. 30 nm of GaN grown at 540°C (to form a nucleation layer) followed by approximately 5 μm of GaN grown at 1020 °C. Trimethylgallium, trimethylindium and ammonia were used as precursor sources of gallium, indium and nitrogen, with hydrogen as the carrier gas for GaN buffer layer growth and nitrogen for InGaN/GaN growth. A 10-period QW structure was grown on top of the pseudo-substrate. Each InGaN QW was grown at 745 °C for 216 s, followed by 2 s of low temperature GaN cap deposition and a 94 s ramp to 860 °C, where it was held until about the GaN barrier was about 7.5 nm thick. X-ray diffraction

measurements on this sample using the method of Vickers *et al.*[21], showed (2.2 ± 0.1) nm QWs with (17.5 ± 1.0) % indium fraction and GaN barriers of (7.5 ± 0.1) nm thickness.

The marker strategy used here is based on the standard in-situ lift-out procedure for high-quality TEM lamellae preparation[22]. In this process, a protective layer of platinum is deposited over the region of interest by electron-beam-induced deposition and then ion-beam-induced-deposition. Typically, a 10 – 20 μm by 2 μm area is masked off. The material either side of the lamella is them milled away with a staircase profile, undercut with a U-shaped milling pattern, secured to a micromanipulator needle and cut free of the bulk material. The sample is then transferred and mounted onto to a TEM half-grid. Finally, the lamella is thinned and polished to electron transparency with the ion beam, using progressively lower ion beam currents and voltages (though further post-FIB argon polishing may also be used).

The defects in the samples examined here have been previously characterised by correlated atomic force microscopy (AFM) and scanning electron microscopy cathodoluminescence (SEM-CL) to identify suitable trench defects for further examination by diffraction contrast TEM, high-angle annular-dark-field scanning TEM (STEM-HAADF) and energy dispersive X-ray spectroscopy (STEM-EDX). The FIB-SEM preparation was carried out in an FEI Helios NanoLab dual-beam microscope (now Thermo Fisher Scientific). STEM/TEM imaging and STEM-EDX was conducted in an FEI Tecnai Osiris microscope operating at 200 kV. The AFM image in Figure 4 was recorded on a Veeco (now Bruker) Dimension 3100 microscope with a Nanoscope V controller in intermittent contact mode.

The site-specific marker method presented here involves two alterations to the standard lift-out process: firstly, fabrication of the initial cross marker and, secondly, monitoring the marker positions during final thinning. The monitoring of the marker positions on the cross-sectional faces during the final thinning steps is shown schematically in Figure 1 (and discussed in more detail below). To produce the markers, the relevant region was identified in the electron beam image and marked with a cross of EBID platinum, with the cross arms long enough to extend outside the footprint to be covered by the protective platinum strap. The cross arms are deposited at ± 45 degrees to the desired long / short axes of the final lamella, and this orientation is determined by the desired crystallographic direction down which the final TEM sample will be viewed. In this sample, the crystallographic orientation was confirmed by checking the orientation of the surface steps in the AFM. The step orientation is determined by the miscut direction of the substrate, which is known relative to the crystallographic axes. The two lines making up the cross were deposited one at a time to allow any charging or drift-

based movement to be corrected, with the ROI at the centre. While the exact deposition parameters can be varied, depositing each line for several seconds using an electron beam energy and current of 5 keV and 0.34 nA respectively gave thin, clear lines sufficiently tall to be seen in cross section during the thinning stages. If, after depositing the marker, any offset between the marker position and the ROI centre is observed, it can be measured and subsequently corrected for during the final thinning steps.

Once the cross marker was formed, the in-situ lift-out process proceeded using the standard methods to mount the relevant sample material on a TEM half-grid[22]. For the protective strap, a 10 μm by 2 μm rectangle pattern of EBID platinum was deposited (typically using a 3 keV electron beam) to form a layer several hundred nanometres thick. This was followed by a further 2 μm thick layer of platinum deposited over the same footprint using ion-beam-induced deposition. The ROI was positioned 3 μm from the end of the platinum strap to reduce the volume of material which would need to be milled away in the thinning process. After covering the region of interest, the lamella could be milled out of the bulk material, transferred with a micromanipulator to a TEM half-grid and secured with platinum ready for the final thinning stages.

Once the redeposited material had been removed, the cross arms were visible as humped features where they met the milled sidewalls. The cross material appeared darker than the protective strap in secondary electron contrast despite them both being EBID platinum, so they could clearly be discerned. This is likely due to differences in the platinum quality and levels of carbon contaminants between the two deposited structures. The central point between the arms indicated the position of the ROI and, for a square cross with arms at 45° to the lamella's long axis, the half-spacing is equal to the distance of the ROI from the milled facet. Accordingly, as the thinning of the final lamella progresses (as shown schematically from stage 1 to 4 in Figure 1) the dark markers on the cross sections are seen to converge.

In the standard FIB preparation process, lamellae are thinned alternately from glancing angles on the front and back sides (using small stage tilts) at progressively lower ion beam currents (and voltages). Here, however, each side was thinned down from the 'front', using the same glancing angle offsets but manipulating the stage so the marker convergence on each side could be monitored with regular electron beam snapshots. While this method is intended to allow a region without strong contrasting features to be centred in a lamella, any small contrasting features (such as the approx. 40 nm deep trenches here) can be used, if present, to fine tune the thickness to help avoid projection effects, if

necessary. Correctly locating these trench edges and differentiating them from the surrounding dislocation-associated V-pits[23] would have been very challenging without any markers. Once the sample was sufficiently thin, a final low-voltage ion beam polishing step was performed to reduce the thickness of the amorphous surface layers, ready for imaging of each previously identified / characterised feature by TEM/STEM.

Results and discussion

The progression of a small trench defect through the marking and lamella preparation procedure is shown in Figure 2. This defect was chosen for further investigation after previous AFM and SEM-CL observations showed it to have interesting properties relative to the surrounding trench defect population. The chosen defect is seen in the centre of subfigure (a), as the ring-shaped feature adjacent to carbon contamination from prior directly correlated SEM-CL imaging. Other trench defects are visible as dark rings and V-pits (inverted hexagonal pyramidal pits associated with threading dislocation terminations in QWs) are visible as dark spots. The chosen defect is seen marked with the platinum cross in (b) and covered with protective EBID platinum in (c). After cutting the ROI free from the bulk material and lifting out the lamella, the appearance of the marker cross in cross-section can be seen in (d) on the rear side of the sample early in the thinning process. This is roughly equivalent to stage 2 of the schematic in Figure 1. As thinning progressed the marker spots began to converge in (e) (roughly equivalent to stage 3 of the schematic in Figure 1) and in the zoomed in subfigure (f) the edge of the trench surrounding the enclosed QWs of interest started to become visible beneath the marker position. The slight offset of marker position and trench position was noted at the deposition stage and could be accounted for during the thinning process. Throughout (d)-(f) the contrast between the deposited lines of the cross arms and the covering EBID platinum strap is clear, despite both being produced by EBID deposition from the same GIS input. This allowed the position of the ROI beneath the thinning surfaces to be carefully monitored and centralised as the thinning progressed.

The final sample at the end of the FIB-SEM process is shown in Figure 3, ready for further analysis in the TEM. Zooming in on the ROI (in the inset image) shows the small trench defect was successfully isolated in the film without the surrounding material to cause projection effects. The contrast between the cross arms and the covering strap is less clear once the sample becomes very thin and bright, but still visible. Sufficient contrast was available to prepare this sample, but the use of differing materials for the cross and EBID strap could increase the contrast in the latter thinning stages if needed.

Figure 4 shows the trench defect imaged by STEM-HAADF (Figure 4(b)) and dark field (DF) TEM (Figure 4(c), with **g** = 1-100), along with the AFM topography of the same defect on the wafer surface prior to FIB preparation (Figure 4(a)). The FIB lamella was lifted out with its long axis perpendicular to the surface step edges visible in the AFM image. The InGaN QWs (brighter in the STEM-HAADF image 4(b)) are discontinuous outside the material enclosed by the trench defect which is characteristic of the InGaN growth method used for this sample (sometimes referred to as ~Q2T growth[24]). The dark contrast of the initiating BSF and the stacking mismatch boundary are clearly visibly in DF TEM (Figure 4(c)), and the QWs from the material enclosed by the defect are clearly seen in Figure 4(b), free from projection effects (as can be confirmed from the trench positions). By allowing a TEM sample to be prepared from previously characterised material, bisecting a region approximately 60 nm wide at the surface containing only enclosed QWs, the subsurface structure and composition (by STEM-EDX) could be compared with previous luminescence and morphological measurements to answer questions not accessible with isolated techniques (the results of which will be published separately). This method is particularly suited to the carrying over of previously characterised features or regions as it does not rely on features being readily identifiable during thinning. In fact, if an interesting region was identified by its electrical behaviour in scanning probe techniques or luminescence behaviour in SEM-CL, the surface cross marker could be deposited over the region of interest by identifying the surrounding topography (which could include marker structures fabricated by a lithographic process) or from the position of carbon contamination left by SEM-CL scans and the region prepared and centred in a TEM lamella for further investigation without any obvious SEM contrast from the region itself.

Though the method successfully allowed defects to be centred in a TEM lamella during manual thinning, there were a few limitations to the approach. As mentioned above, the contrast between the cross arms and the surrounding EBID platinum was harder to discern at small thicknesses. The use of different marker and strap materials here may prolong the contrast during thinning. Secondly, rotating the sample to monitor the thinning on both sides is more time consuming than the standard preparation procedure, so this approach is best suited to the preparation of features which are either particularly rare or have been pre-characterised in such detail that successful preparation of a high quality sample with a low failure rate becomes crucial. Finally, the marker resolution is limited by the line thickness and the overlap of the two cross arms. If sample drift is not an issue, an X-mark could be deposited directly rather than two overlapping lines, which would have a thinner overlap at the centre. Thinner lines can also be deposited, down to sub 20 nm structures [25,26]. Thinner lines would, however, be harder to see, so the width should be matched to the accuracy needed, with sufficient

height to be seen in cross section and sufficiently low drift / charging to prevent smearing of the deposition.

This method has been demonstrated here on one type of defect in one material system, but the process is not defect- or material-specific. This approach is equally applicable to any number of defects in the III-nitrides where low cross-sectional contrast makes centring them in a FIB lamella more challenging, and the deposition-based markers should easily transfer to other materials systems as well, and to the deposition of other materials from other GIS inputs. In addition, using these markers to centre small features in a sub-100 nm region could be equally helpful to prepare APT needle samples containing low-contrast features, with the markers visible on the curved sidewall of the thinning needle. As the markers are directly above the region of interest (and are at the bottom of the protective platinum layers) they could be preserved until the final stages of APT needle preparation when the last of the protective platinum cap is removed.

Conclusions

The marker method presented here allows the precise location of a region of interest or of previously characterised material throughout FIB-SEM preparation of TEM lamellae, using markers produced solely by deposition. This was demonstrated here by the preparation of a FIB lamella bisecting a previously characterised small trench defect (less than 100 nm wide at the surface), allowing TEM and STEM-HAADF images free from projection effects to be correlated with previous AFM measurements.

No additional damage is introduced to the sample over that in the standard in-situ lift-out process, and the depth of the ROI below each milled sidewall could be monitored and the thinning parameters adjusted accordingly. This method is particularly useful for objects with small or no contrast features on the lamellar cross section which would otherwise be difficult to locate during the thinning process. It is particularly applicable to directly correlated multi-microscopy investigations where a small number of precisely located samples must be prepared. Though this method was demonstrated here on a defect in GaN, the process should transfer well to a wide range of material systems where the location of features in cross-section is difficult to achieve.
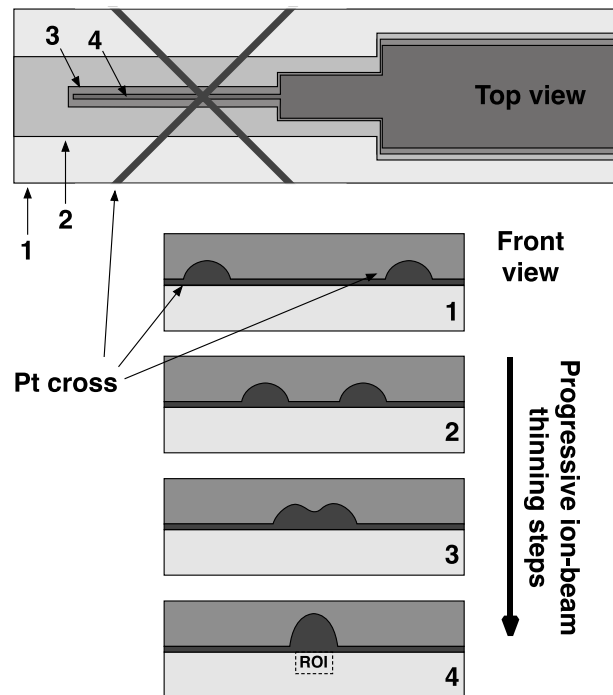
Acknowledgements

Figures

Figure 1 – Schematic illustration of the marker appearance throughout the progressive ion-beam thinning process. At the start of the final thinning (stage 1) the cross arms are visible on each cross section as two widely spaced, dark, humped features. As the thinning proceeds on both the front and back faces (moving to stage 2, then stage 3) the markers on the cross section move closer together. Smaller milling windows are used for the lower ion beam currents, as shown in the top view. Finally, as the lamella nears its final thickness, the dark features on the cross section converge into a single raised marker above the ROI (stage 4).
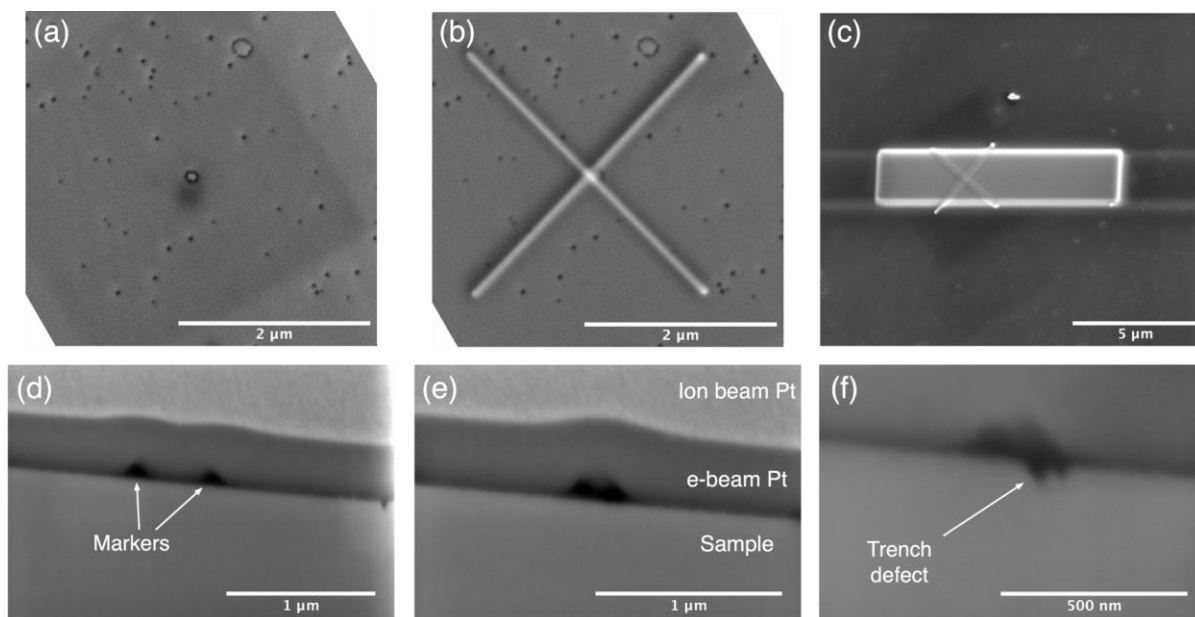
Figure 2 – Secondary electron images of the cross marker procedure in the FIB-SEM. A small trench defect (centred in (a)) is marked with a cross of EBID platinum in (b), which is subsequently covered by the EBID platinum strap in (c). Subfigures (d-f) show the close-up monitoring of the markers on the lamellar cross section during final thinning on the TEM grid, after the lift-out process. The two dark marks from the cross arms are seen to converge from (d-f) as the lamella is thinned (with subfigure (f) at a higher magnification than (d) & (e)).
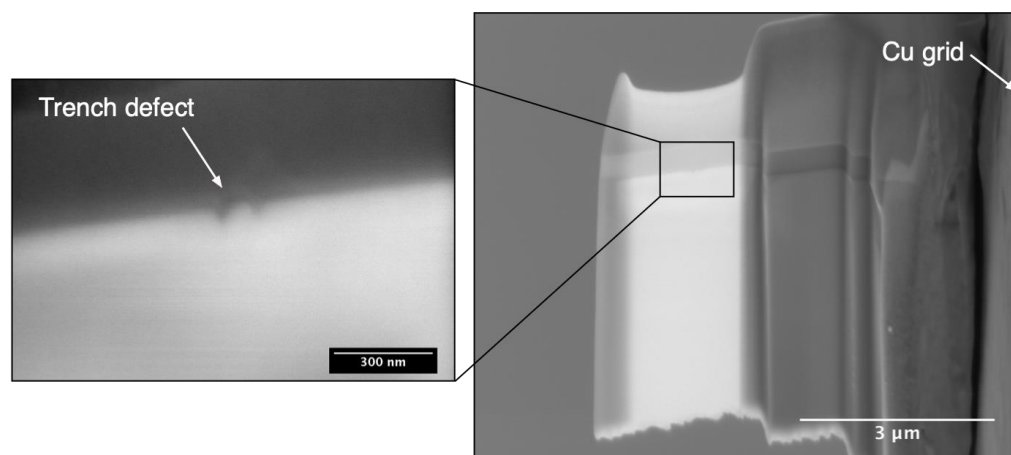

Figure 3 – The trench defect is just visible at high magnification and contrast in the final lamella, seen in secondary electron contrast in the FIB-SEM. The bright appearance of the lamella is characteristic of very thin material in the FIB-SEM.
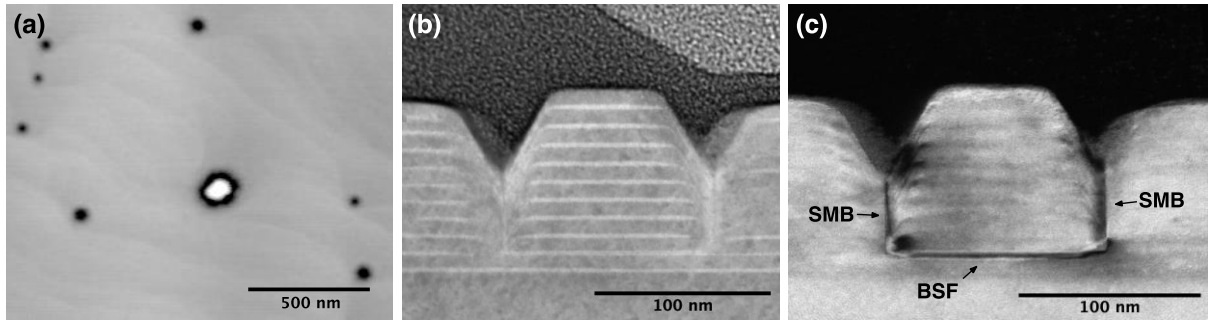
Figure 4 – The exact same trench defect seen in plan-view in the AFM (a), and in cross-section by STEM-HAADF (b) and DF TEM (c). Images (b) and (c) are viewed close to the <11-20> zone axis, with the DF image taken with **g** = 1-100. V-pits (seen as black hexagonal pits) and surface steps are also visible in the AFM image. The InGaN QWs are visible with bright contrast in the STEM-HAADF image (b) and the BSF and SMB are seen as dark features in (c).

References

1. Mayer, J., Giannuzzi, L. A., Kamino, T. & Michael, J. TEM Sample Preparation and FIB-Induced Damage. *MRS Bull.* **32**, 400–407 (2007).

2. Scholder, O. *et al.* Helium focused ion beam fabricated plasmonic antennas with sub-5 nm gaps. *Nanotechnology* **24**, (2013).

3. Thompson, K. *et al.* In situ site-specific specimen preparation for atom probe tomography. *Ultramicroscopy* **107**, 131–139 (2007).

4. Tang, F. *et al.* Practical Issues for Atom Probe Tomography Analysis of III-Nitride Semiconductor Materials. *Microsc. Microanal.* **21**, 544–556 (2015).

5. Babinsky, K., De Kloe, R., Clemens, H. & Primig, S. A novel approach for site-specific atom probe specimen preparation by focused ion beam and transmission electron backscatter diffraction. *Ultramicroscopy* (2014).

6. Lozano-Perez, S. A guide on FIB preparation of samples containing stress corrosion crack tips for TEM and atom-probe analysis. *Micron* (2008).

7. Mancini, L. *et al.* Multi-microscopy study of the influence of stacking faults and three-dimensional In distribution on the optical properties of m-plane InGaN quantum wells grown on microwire sidewalls. *Appl. Phys. Lett.* **108**, 042102 (2016).

8. Massabuau, F. C.-P. *et al.* Correlations between the morphology and emission properties of trench defects in InGaN/GaN quantum wells. *J. Appl. Phys.* **113**, 073505 (2013).

9. Dai, J. Y. *et al.* Development of a rapid and automated TEM sample preparation method in semiconductor failure analysis and the study of the relevant TEM artifact. *Microelectronics J.* **32**, 221–226 (2001).

10. Van Leer, B. & Giannuzzi, L. A. Advances in TEM sample preparation using a focused ion beam. *Microsc. Microanal.* **14**, 380–381 (2008).

11. Reyes, R. *et al.* Automated SEM and TEM sample preparation applied to copper/low k materials. in *AIP Conference Proceedings* vol. 550 580–585 (AIP, 2001).

12. Langford, R. M. & Rogers, M. In situ lift-out: Steps to improve yield and a comparison with other FIB TEM sample preparation techniques. *Micron* **39**, 1325–1330 (2008).

13. Pettersson, H., Nik, S., Weidow, J. & Olsson, E. A method for producing site-specific tem specimens from low contrast materials with nanometer precision. *Microsc. Microanal.* **19**, 73–78 (2013).

14. Prosa, T. J. & Larson, D. J. Modern Focused-Ion-Beam-Based Site-Specific Specimen Preparation for Atom Probe Tomography. *Microsc. Microanal.* **23**, 194–209 (2017).

15. Thermo Fisher Scientific. AutoTEM 4 Datasheet: DS0242-EN-07-2017. https://assets.thermofisher.com/TFS-Assets/MSD/Datasheets/AutoTEM-4-Datasheet.pdf (2017).

16. Sugahara, T. *et al.* Direct Evidence that Dislocations are Non-Radiative Recombination Centers in GaN. *Jpn. J. Appl. Phys.* **37**, 398–400 (1998).

17. Liu, R. *et al.* Luminescence from stacking faults in gallium nitride. *Appl. Phys. Lett.* **86**, 021908 (2005).

18. Rigutti, L. *et al.* Correlation of microphotoluminescence spectroscopy, scanning transmission electron microscopy, and atom probe tomography on a single nano-object containing an InGaN/GaN Multiquantum well system. *Nano Lett.* **14**, 107–114 (2014).

19. Massabuau, F. C.-P. *et al.* Carrier localization in the vicinity of dislocations in InGaN. *J. Appl. Phys.* **121**, (2017).

20. Massabuau, F. C.-P. *et al.* Morphological, structural, and emission characterization of trench defects in InGaN/GaN quantum well structures. *Appl. Phys. Lett.* **101**, 212107 (2012).

21. Vickers, M. E. *et al.* Determination of the indium content and layer thicknesses in InGaN/GaN quantum wells by x-ray scattering. *J. Appl. Phys.* **94**, 1565 (2003).

22. Schaffer, M., Schaffer, B. & Ramasse, Q. Sample preparation for atomic-resolution STEM at low voltages by FIB. *Ultramicroscopy* **114**, 62–71 (2012).

23. Shiojiri, M., Chuo, C. C., Hsu, J. T., Yang, J. R. & Saijo, H. Structure and formation mechanism of V defects in multiple InGaN/GaN quantum well layers. *J. Appl. Phys.* **99**, 073505 (2006).

24. Massabuau, F. C.-P. *et al.* Investigation of unintentional indium incorporation into GaN barriers of InGaN/GaN quantum well structures. *Phys. status solidi* **252**, 928–935 (2015).

25. Hari, S., Verduin, T., Kruit, P. & Hagen, C. W. A study of the reproducibility of electron beam induced deposition for sub-20 nm lithography. *Micro Nano Eng.* **4**, 1–6 (2019).

26. Durrani, Z. A. K., Jones, M. E., Wang, C., Scotuzzi, M. & Hagen, C. W. Electron transport and room temperature single-electron charging in 10 nm scale PtC nanostructures formed by electron beam induced deposition. *Nanotechnology* **28**, (2017).